https://doi.org/10.5194/egusphere-2026-6471
Preprint. Discussion started: 16 November 2026
© Author(s) 2026. CC BY 4.0 License.

Fundamental trade-off between climate and air quality from sulfur reductions in shipping fuels

Liliane Isselhorst[1], Mattia Righi[1], Anja Schmidt[1,2], Johannes Hendricks[1], and Axel Lauer[1]

[1]Deutsches Zentrum für Luft- und Raumfahrt (DLR), Institut für Physik der Atmosphäre, Oberpfaffenhofen, Germany
[2]Meteorological Institute, Ludwig-Maximilians-University of Munich, Munich, Germany

Correspondence: Liliane Isselhorst (liliane.isselhorst@dlr.de)

Abstract. International shipping is a major source of sulfur emissions. Combustion of marine fuels with high fuel sulfur content (FSC) releases SO_2, promoting sulfate aerosol particle formation. These particles cool the climate by enhancing cloud albedo and reflecting solar radiation, but harm air quality and human health. In 2020, the IMO2020 regulation reduced the global FSC limit from 3.5% to 0.5%, decreasing sulfate aerosol burdens and their cooling effect, uncovering previously masked anthropogenic warming. Using a global aerosol–climate model, we quantify the loss of cooling and explore alternative emission scenarios that could preserve aerosol-induced cooling while improving air quality. Without IMO2020, model-simulated shipping-induced aerosol effective radiative forcing is -112 mW m^{-2} globally. IMO2020 regulations reduce this cooling by 67 mW m^{-2} and ship-induced $PM_{2.5}$ concentrations decrease on average by 57% across the world's most populous coastal cities. Sensitivity simulations show that enforcing IMO2020 regulations in coastal regions yields the greatest air quality benefits, whereas regulations over the open-ocean have little impact. However, coastal FSC reductions also account for the largest loss of cooling, consistent with the combination of dense ship traffic and high cloud albedo susceptibility to changes in aerosol concentrations. Retaining pre-IMO2020 FSC in regions with at least 30% mean low-cloud cover could mitigate this loss of cooling but at the cost of limited air quality improvements in some areas. Our findings highlight the trade-off between reducing shipping-induced air pollution and preserving aerosol-induced cooling. Future research should further assess this trade-off considering additional alternative fuels.

1 Introduction

International shipping is the second-largest emitter of greenhouse gases (GHGs) within the transport sector, accounting for 9% (0.8 Gt CO_2-eq) of total transport-related GHG emissions in 2019 (Jaramillo et al., 2022). Besides GHGs, in particular CO_2, ships emit various short-lived climate forcers (SLCFs), like nitrogen oxides (NO_x), CO, non-methane volatile organic compounds (NMVOC), SO_2 and aerosol particles such as black and organic carbon (BC and OC) and sulfate (SO_4). These aerosol particles and reactive chemical compounds significantly affect the Earth's radiation budget and the environment, while also deteriorating air quality, thus posing a risk to human health (Szopa et al., 2021; Pope and Dockery, 2006).

This study focuses on sulfur emissions and sulfate aerosol particles from international shipping. Until the recent introduction of more stringent regulations, most ships used heavy fuel oil (HFO) as their main fuel, which is characterized by a very high

https://doi.org/10.5194/egusphere-2026-6471
Preprint. Discussion started: 16 November 2026
© Author(s) 2026. CC BY 4.0 License.

FSC (about 2.6% by mass in 2018; Faber et al., 2021). As a consequence, global shipping contributed about 12% (12 Tg) to global anthropogenic SO_2 emissions in 2019 (Yi et al., 2025). The large majority of the sulfur contained in ship fuels is released as gaseous SO_2 that is then oxidized in the atmosphere to sulfuric acid (H_2SO_4) vapour, which in turn nucleates to form new sulfate aerosol particles and/or condenses onto existing aerosol particles (Seinfeld and Pandis, 2016). These sulfate aerosol particles can act as additional CCN enhancing the formation of cloud droplets. This in turn affects cloud microphysical and optical properties as well as cloud lifetime (Twomey, 1977; Albrecht, 1989). As a result of the more numerous but smaller-sized droplets – and under the assumption that the liquid water content of the cloud remains unchanged – cloud albedo increases (i.e., clouds become brighter), which causes a negative effective radiative forcing (ERF) due to the increased reflection of solar radiation (Twomey, 1977). The effect of aerosol-cloud interactions in shipping is well-known and evident, for instance, in satellite images of ship tracks, known as ship tracks, formed behind ships (Schreier et al., 2007; Watson-Parris et al., 2022). According to recent estimates, globally-averaged, shipping-induced ERF amounts to -146 mW m^{-2} including the effect of both aerosol-radiation interactions and aerosol-cloud interactions for the year 2015 (Hendricks et al., 2026). Earlier studies reported stronger cooling effects, with total aerosol ERF estimates ranging from about -600 to -390 mW m^{-2}, depending on the simulation year and model configuration. Specifically, Lauer et al. (2009), Eyring et al. (2010), and Partanen et al. (2013) estimated total shipping-induced ERFs of -600 mW m^{-2} for 2012, -400 mW m^{-2} for 2005, and -390 mW m^{-2} for 2010, respectively.

Aerosol particles from shipping also affect air quality and thus human health. Sofiev et al. (2018) estimated that approximately 400,000 premature cardiovascular disease and lung cancer deaths can be attributed to ship emissions in 2020 assuming no regulations regarding the FSC. Specifically, particulate matter (PM) with diameter smaller 2.5 μm ($PM_{2.5}$) is harmful to human health (Pope and Dockery, 2006). Mortality rates are especially high in densely populated port areas and coastal regions with high shipping activity, e.g. in Europe and Asia (Corbett et al., 2007).

In order to improve air quality by reducing sulfur and PM emissions from shipping, the IMO introduced global emission control measures under Annex VI of MARPOL (The International Convention for the Prevention of Pollution from Ships). In addition, even stricter limits have been imposed at the regional level within several Emission Control Areas (ECAs). Ships entering ECAs must use low-sulfur fuel or operate wet scrubbers to remove sulfur compounds from the exhaust gases when burning fuels with higher sulfur content (Buhaug et al., 2009). So far, ECAs have been established in the Baltic Sea, the North Sea, along the western and eastern coasts of North America, and in the United States Caribbean sea area (Fig. S1). Recently, the ECAs in the Canadian Arctic and the Norwegian Sea were enforced (International Maritime Organization, 2024), however these are not included in our analysis. In the future, further areas covering e.g. the North-East Atlantic are expected to be designated as ECAs (Faber et al., 2021). Fig. 1 shows the FSC limitation introduced by the IMO from 2008 to 2022. Until 2010, the FSC limit in ECAs (blue line) was 1.5%, which until the end of 2014 was then further decreased to 1%. From 2015 onwards, the maximum FSC in ECAs was limited to 0.1%. Outside ECAs, the maximum allowable FSC was 4.5% until 2012 was subsequently lowered to 3.5% until 2020 (Buhaug et al., 2009), although the global average FSC of the fleet was already below this limit (2.6%). In January 2020, a new regulation known as IMO2020 was implemented, which drastically reduced

https://doi.org/10.5194/egusphere-2026-6471
Preprint. Discussion started: 16 November 2026
© Author(s) 2026. CC BY 4.0 License.

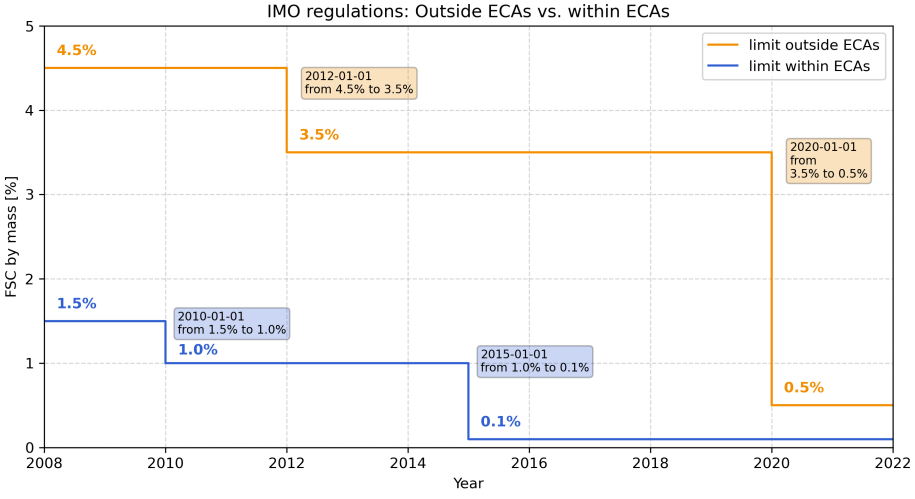


Figure 1. Historical development of FSC limits imposed by the IMO for ships operating outside and within ECAs.

the FSC of ships operating outside ECAs from 3.5% to 0.5%, in order to further reduce environmental damage and risks to human health caused by ship emissions (Faber et al., 2021).

The IMO fuel-sulfur regulations were primarily introduced to protect the environment, i.e. to improve air quality. However, they also reduced the cooling effect of sulfate aerosols from ship emissions. This loss of aerosol cooling refers to the weakening of the net negative ERF from ship emissions, which had previously masked part of the global warming. Several recent studies have quantified the loss of aerosol cooling caused by the IMO2020 regulations. These studies can be grouped into three categories according to their methodological approach: single-model studies (Partanen et al., 2013; Sofiev et al., 2018; Bilsback et al., 2020; Yuan et al., 2022; Hausfather and Forster, 2023; Gettelman et al., 2024; Yoshioka et al., 2024) reported a loss of cooling ranging from 27 to 330 mW m^{-2}. The multi-model study by Skeie et al. (2024) estimated a loss of cooling of 73 mW m^{-2}, whereas observational studies (Diamond, 2023; Hansen et al., 2025) found values between 100 and 500 mW m^{-2} (see Fig. 4). These different estimates highlight that the effect of the IMO fuel-sulfur regulations on the aerosol cooling from ship emissions remains a topic of ongoing scientific debate. As maritime trade is expected to expand further in the future (UNCTAD, 2024), it is crucial to fully understand the consequences of marine emission regulations on climate and air quality. Additionally, assessing the loss of aerosol cooling due to the IMO regulations is critical for better understanding the viability and risks of geoengineering strategies like marine cloud brightening, which aims to reduce anthropogenic global warming by brightening marine stratocumulus clouds through atmospheric injection of aerosols (Yuan et al., 2024). Warm low-level clouds, especially marine stratocumulus, are particularly relevant in our study: they cover large areas of the subtropical oceans and account for a substantial fraction of the global cooling effect of the short-wave cloud forcing (Chen et al., 2000).

In this work, we investigate the loss of aerosol cooling from international shipping due to IMO2020 regulations and also analyze the change in PM concentrations using a state-of-the-art global aerosol-chemistry-climate model (Righi et al., 2023).

https://doi.org/10.5194/egusphere-2026-6471
Preprint. Discussion started: 16 November 2026
© Author(s) 2026. CC BY 4.0 License.

While numerous studies have assessed the loss of aerosol cooling associated with IMO2020, only a few have considered the climate and air-quality impacts of sulfur reductions simultaneously. For instance, Partanen et al. (2013) investigated both aspects in different fuel-sulfur scenarios, including reduced sulfur emissions near continents combined with higher sulfur emissions over the open ocean, as well as a scenario approximately representing the IMO-2020 regulations. Sofiev et al. (2018) similarly assessed both the air-quality and climate impacts of the IMO-2020 sulfur regulations by comparing projected 2020 ship emissions with and without implementation of the 0.5% FSC limit and evaluating changes in PM2.5-related premature mortality and aerosol ERF. We extend the approach of Partanen et al. (2013) by considering the role of low-level cloud cover. In addition to the analysis of IMO2020 and a scenario in which a higher FSC is retained in the open ocean while IMO-compliant low FSC is applied in coastal regions, we look at three scenarios in which higher FSC is only permitted in regions exceeding different thresholds of climatological low-level cloud-cover fraction. For each scenario we quantify the loss of cooling and the ship-induced impact on the large-scale $PM_{2.5}$ concentration in coastal areas and discuss the trade-off between the two in terms of climate effects and air quality impacts. The goal is to assess whether it is possible to improve air quality while simultaneously preserving the cooling effect induced by shipping aerosols.

2 Emissions setup and model simulations

The model simulations in this study are performed with the EMAC model (ECHAM/MESSy Atmospheric Chemistry) using the model configuration by Righi et al. (2023), which has been applied in several studies for assessing the impact of transport emissions on aerosols and climate. EMAC is a chemistry-climate model combining several submodels to simulate tropospheric and middle-atmospheric processes, including interactions with oceans, land, and anthropogenic influences (Jöckel et al., 2016). Built on the Modular Earth Submodel System v2 (MESSy; Jöckel et al., 2010), it uses ECHAM5 as its core atmospheric general circulation model (Roeckner et al., 2006). Aerosol microphysics is simulated by the submodel MADE3 (Modal Aerosol Dynamics for Europe adapted for global applications, third version; Kaiser et al., 2014) with nine log-normally distributed aerosol species representing three size classes and mixing states. Its performance has been evaluated with data from global observational networks, aircraft-based field campaigns, and satellites (Kaiser et al., 2019). Cloud processes are handled by the submodel CLOUD, accounting for aerosol effects on warm, mixed-phase, and cirrus clouds using a two-moment cloud microphysics scheme (Kuebbeler et al., 2014). Aerosol-radiation and cloud-radiation interactions are explicitly represented via the RAD and CLOUDOPT submodels (Dietmüller et al., 2016). To isolate the aerosol effects, radiatively active gases (CO_2, CH_4, N_2O, O_3, and chlorofluorocarbons) are prescribed using globally averaged values and an ozone climatology. The model resolution is T42L41 ($\sim 2.8° \times 2.8°$, ~300 km at the Equator) with 41 vertical levels extending from the surface to 5 hPa. The simulations cover the time period 2010-2020 (11 years), with the first year excluded as spin-up. Meteorology is nudged using ERA5 reanalysis data (Hersbach et al., 2020). Further details on the model configuration can be found in Righi et al. (2023).

Compared to Righi et al. (2023), a different emission setup is used here to better account for the effects of the shipping emission regulations. Instead of using the CMIP6 emission inventory (Gidden et al., 2019), emission data for this work are taken from the Copernicus Atmosphere Monitoring Service (CAMS) global emission inventory for anthropogenic emissions (Soulie

https://doi.org/10.5194/egusphere-2026-6471
Preprint. Discussion started: 16 November 2026
© Author(s) 2026. CC BY 4.0 License.

Table 1. Overview of the simulations performed in this study and the corresponding annual emissions of the most relevant species. An additional baseline simulation (BASE) without shipping emissions is used to quantify the shipping effects with the perturbation method. For the definition of ocean/coastal regions and the cloud masks see Figs. S2 and S3 in the supplement. Emissions are in units of Tg(species), Tg(NO) for NO_x, and 10^{25} for particle number (N_{aer}). Particulate organic matter (POM) emissions are calculated as 1.4 times OC emissions.

Simulation	Ship emissions	CO_2	NO_x	SO_2	SO_4	BC	POM	N_{aer}
IMO-2020	CAMS 2020	824	10.5	2.0	0.13	0.012	0.24	9.4
PRE-IMO	CAMS 2010 scaled to 2020 activity	824	12.1	10.0	0.55	0.029	0.44	24.0
PRE-IMO-OCEAN	CAMS 2010 scaled to 2020 activity (open ocean only)	824	10.6	3.4	0.20	0.015	0.27	11.7
PRE-IMO-CLOUD30	CAMS 2010 scaled to 2020 activity (where clouds $> 30\%$)	824	10.8	4.2	0.24	0.017	0.30	13.3
PRE-IMO-CLOUD40	CAMS 2010 scaled to 2020 activity (where clouds $> 40\%$)	824	10.6	2.9	0.17	0.014	0.26	10.9
PRE-IMO-CLOUD50	CAMS 2010 scaled to 2020 activity (where clouds $> 50\%$)	824	10.5	2.3	0.14	0.013	0.25	9.8
BASE	No ship emissions	–	–	–	–	–	–	–

et al., 2024), integrated with the Global Fire Assimilation System (GFAS) 1.2 dataset for biomass burning emissions (Copernicus Atmosphere Monitoring Service, 2022). The dataset used for the ship emissions is the CAMS-GLOB-SHIP version 3.2 with a spatial resolution of $0.1^\circ \times 0.1^\circ$ and a monthly temporal resolution. CAMS-GLOB-SHIP is generated by the Ship Traffic Emission Assessment Model (STEAM v4.1; Johansson et al., 2017) and provides spatially-resolved fuel consumption and emissions of CO_2, CO, NO_x, NMVOCs, BC, OC, SO_x and SO_4. For the purpose of this work, it is assumed that SO_x is emitted in form of SO_2. The CAMS shipping emissions for the years 2014-2021 are based on observed vessel activity from the terrestrial and satellite-based Automated Identification System (AIS), while for the years 2000-2013, the data are derived by backcasting the 2016 vessel activity assuming certain changes in the energy efficiency of the vessels, number of vessels and smaller average ship sizes in the past. Thanks to the detailed information on the global shipping activity and fuel consumption, this inventory can account for the impact of socioeconomic disruptions, such as the COVID-19 pandemic or the introduction of emission regulations, including the IMO regulations, and is therefore particularly suitable for this study.

Several simulations are performed to quantify the impact of shipping on climate and air quality after the introduction of the IMO2020 regulations and in several emissions scenarios representing pre-IMO2020 conditions (Table 1). The goal is to isolate the impact of the IMO2020 regulations and to explore possibilities how these could be adjusted to potentially minimize the trade-off between air quality improvements and inadvertent climate warming following the reduction of shipping-induced cooling. The reference simulation is IMO-2020 and represents shipping emissions under full compliance with the IMO2020 regulations, which limit the FSC to 0.5% globally and to 0.1% within ECAs. It reflects real-world conditions in 2020 and is used to assess the actual impact of regulated shipping emissions on climate and air quality. In this simulation, the annual global ship emissions of SO_2 amount to 2.0 Tg, with additional 0.13 Tg emitted in form of primary SO_4.

For comparison, the impact of shipping prior to the IMO2020 regulations is assessed in the PRE-IMO simulation: it represents a hypothetical case in which no sulfur regulations were implemented. It uses 2010 emissions for all shipping-related species with a FSC limit of 4.5% globally and 1% within ECAs, scaled to 2020 shipping activity. This scaling is realized using

https://doi.org/10.5194/egusphere-2026-6471
Preprint. Discussion started: 16 November 2026
© Author(s) 2026. CC BY 4.0 License.

CO_2 emissions as a proxy for activity as the CO_2 emission factor can be assumed constant (about 3.2 $kg_{CO_2}\ kg_{fuel}^{-1}$). The emissions of each species X are then calculated as:

$$X_{2020} = X_{2010}\,\frac{CO_2^{2020}}{CO_2^{2010}}, \tag{1}$$

with the scaling factor CO_2^{2020}/CO_2^{2010} = 1.02. This results in much higher annual global shipping emissions of SO_2 and SO_4 compared to IMO-2020: 10.0 Tg and 0.55 Tg, respectively, with large increases also for the other species, while CO_2 emissions remain constant at 824 Tg.

In the PRE-IMO-OCEAN simulation a similar scaling is applied to open-ocean regions only, while the IMO2020 values are retained in coastal areas. The latter are defined based on the Exclusive Economic Zones, roughly covering coastal waters within 200 nautical miles ($\sim$ 370 km) from the coastlines (Flanders Marine Institute, 2023, see Fig. S2). Analogous to Eq. (3), the emissions of each species X in simulation PRE-IMO-OCEAN are calculated as:

$$X_{2020} = X_{2010}(\text{open ocean})\,\frac{CO_2^{2020}}{CO_2^{2010}} + X_{2020}(\text{coastal}). \tag{2}$$

This simulation is designed to quantify the impact of a partial enforcement of the IMO2020 regulations, with the 0.5% FSC limit applied only in the coastal regions, where impacts on air quality are more relevant, while the 4.5% FSC limit remains on the open ocean, in an attempt to reduce the loss of cooling due to reduced sulfur emissions. The global emissions of SO_2 and SO_4 in this simulation are higher than those in the IMO-2020 case (3.4 Tg and 0.20 Tg, respectively) but lower than those in the PRE-IMO case.

In the PRE-IMO-CLOUD30, PRE-IMO-CLOUD40 and PRE-IMO-CLOUD50 simulations regions where high FSC emissions are released are determined by the climatological average fraction of low-level clouds, since sulfur emissions have a larger climate effect and a stronger cooling impact in regions where the fraction of these clouds is high. The aim is to maintain a strong cooling effect while minimizing impacts on air quality, by specifically targeting climate sensitive regions. For that purpose, we use a climatology of the cloud fraction from ESA Cloud_cci Advanced Very High Resolution Radiometer (AVHRR) for the years 1996-2016 (Stengel et al., 2020) and apply scaled 2010 shipping emissions in the grid-boxes with a climatological low-level cloud fraction $\mathcal{C}$ larger than a given threshold $\hat{\mathcal{C}}$, while 2020 emissions are applied outside these areas:

$$X_{2020} = X_{2010}(\mathcal{C} \geq \hat{\mathcal{C}})\,\frac{CO_2^{2020}}{CO_2^{2010}} + X_{2020}(\mathcal{C} < \hat{\mathcal{C}}) \tag{3}$$

We perform simulations for three different thresholds of 30% (PRE-IMO-CLOUD30), 40% (PRE-IMO-CLOUD40) and 50% (PRE-IMO-CLOUD50), respectively. The resulting cloud cover masks are shown in Fig. S3. The global annual emissions in these simulations vary from 2.3 to 4.2 Tg of SO_2 and from 0.14 to 0.24 Tg of SO_4. Those values are quite close to those for the PRE-IMO-OCEAN simulation, but exhibit a different geographical distribution. At this point, we want to emphasize that our scaling approach assumes that, apart from changes in transport activity, fuel use and ship technology in the selected regions did not change between 2010 and 2020. The scenarios therefore approximate a situation in which 2020 shipping activity occurs with a 2010-like fleet and fuel state. This assumption is plausible given the long turnover times of the shipping fleet. However, differences in emission factors for non-sulfur species between the 2010 and 2020 inventories remain a source of uncertainty.

https://doi.org/10.5194/egusphere-2026-6471
Preprint. Discussion started: 16 November 2026
© Author(s) 2026. CC BY 4.0 License.



As in Righi et al. (2023), the shipping-induced effects on climate and air quality are quantified using the perturbation method. This involves comparing each of the above simulations with a baseline simulation (BASE in Table 1) in which emissions from the shipping sector are set to zero. The effect of the shipping sector in each of the simulations is then calculated as the difference between the sensitivity simulation (SIM) and the BASE simulation. The resulting absolute change A in a specific quantity (e.g., a climate or air quality indicator) due to ship emissions is defined as the difference $A = \mathrm{SIM} - \mathrm{BASE}$. The statistical significance of the signal is evaluated using a paired-sample t-test at the 95% confidence level. The ERF is used as a metric to quantify the climate impact and is calculated as the difference in the top-of-the-atmosphere (TOA) radiative fluxes between the two simulations:

$$\Delta\mathrm{ERF} = F_{\mathrm{SIM}}^{\mathrm{all-sky}} - F_{\mathrm{BASE}}^{\mathrm{all-sky}}. \tag{4}$$

To quantify the fraction of ERF due to aerosol-cloud interactions, the cloud radiative forcing (CRF) is calculated:

$$\Delta\mathrm{CRF} = \left(F_{\mathrm{SIM}}^{\mathrm{all-sky}} - F_{\mathrm{BASE}}^{\mathrm{all-sky}}\right) - \left(F_{\mathrm{SIM}}^{\mathrm{clear-sky}} - F_{\mathrm{BASE}}^{\mathrm{clear-sky}}\right), \tag{5}$$

where $F^{\mathrm{clear-sky}}$ is the (diagnostic) TOA radiative flux calculated by the EMAC radiation scheme with no cloud radiative effects. Note, however, that the clear-sky component cannot be attributed to aerosol-radiation interactions only, as it may also include contributions from other forcings, such as changes in water vapor and the semi-direct effect.

To assess the impact on air quality, we use the ship-induced $PM_{2.5}$ concentration at the surface, i.e. the mass concentration in particles with diameter below 2.5 μm at the lowermost model layer as a metric. $PM_{2.5}$ is calculated from the EMAC model output by adding the mass concentration of each aerosol species i (excluding aerosol water) below a diameter of 2.5 μm. For the lognormal size distributions used by MADE3, this can be expressed as:

$$\mathrm{PM}_{2.5} = \sum_{i,j} m_{i,j} \left[\frac{1}{2} + \frac{1}{2}\mathrm{erf}\left(\frac{\ln(2.5/D_{V,j})}{\sqrt{2}\ln\sigma_j}\right)\right], \tag{6}$$

where $m_{i,j}$ is the mass of the aerosol species i in mode j, σ_j the geometric standard deviation of mode j and $D_{V,j} = \exp\left[\ln(D_j) + 3\ln^2\sigma_j\right]$ the volume median diameter of the mode j given its median diameter D_j in μm.

For the analysis of air quality in coastal regions, we consider the ten most populous coastal cities on each continent with populations larger than one million people (see Fig. S4 in the supplement). These cities provide the basis for assessing $PM_{2.5}$ changes under the different ship emission scenarios. We analyze both, absolute and relative $PM_{2.5}$ concentrations, aggregated at the global and continental scales. Relative $PM_{2.5}$ values represent the contribution of shipping-related $PM_{2.5}$ to the total $PM_{2.5}$.

3 Results

3.1 Climate effects

Figure 2a shows the ship-induced global-mean ERF and CRF for the emission scenarios investigated in this study. The PRE-IMO simulation, representing ship emissions before the implementation of the IMO2020 sulfur regulations, exhibits

https://doi.org/10.5194/egusphere-2026-6471
Preprint. Discussion started: 16 November 2026
© Author(s) 2026. CC BY 4.0 License.

the strongest aerosol cooling with an ERF of -112 ± 16 mW m^{-2}. This is lower than the value of -145 ± 37 mW m^{-2} quantified by Righi et al. (2023) using the same model but with a different emission inventory (CMIP6 for 2015 instead of CAMS for 2020, see Sect. 2). Interestingly, the CRF accounts for 55% of the total effect in this study, while in Righi et al. this fraction was much higher, around 80%. This could be attributed to the much higher BC emissions in CMIP6 (0.17 Tg vs. 0.03 Tg) leading to a stronger warming from aerosol-radiation interactions and, consequently, a less-negative clear-sky ERF. This, in turn results in a larger contribution from CRF dominating the total ERF. The different geographical distributions of the emissions in the two inventories could also play a role, as the CRF depends on the aerosol-cloud interactions between ship-induced particles and low-level clouds.

Following the enforcement of the IMO2020 regulations, which reduced the FSC from 3.5% to 0.5%, the shipping-induced cooling decreases to -45 ± 18 mW m^{-2} in the IMO-2020 simulation. This corresponds to a reduction by a factor of 2.5 compared with PRE-IMO conditions and a loss of cooling of 67 ± 14 mW m^{-2} (Fig. 2b). This loss of cooling can be explained by the 80% lower sulfur emissions from ships in IMO-2020, which decrease the number of available CCN. This leads to lower cloud droplet number concentrations and reduced cloud brightness, i.e. a reversal of the marine cloud brightening (MCB) effect. The reduction, however, is not only in the CRF, indicating that clear-sky effects and changes in the emissions of other species, such as BC, also contribute substantially to the overall response.

The PRE-IMO-OCEAN scenario, in which the IMO2020 regulations are applied only in coastal regions while ships in the open ocean continue to operate on fuels with a PRE-IMO FSC, results in an ERF of -65 ± 19 mW m^{-2}. Maintaining high sulfur emissions over open ocean regions, where low-cloud cover is often high, partially helps to preserve the cooling: compared to the IMO-2020 scenario, the loss of cooling in this experiment is significantly smaller. This motivated further scenarios that specifically target regions of high low-level cloud cover.

Applying PRE-IMO FSC only in regions with a climatological low-level cloud fraction exceeding 40% or 50% does not help to preserve the cooling: both the PRE-IMO-CLOUD40 and PRE-IMO-CLOUD50 simulations result in an ERF which is not significantly different from the IMO-2020 scenario (-45 ± 27 mW m^{-2} and -52 ± 17 mW m^{-2}, respectively) and the loss of cooling shows a similar magnitude. Lowering the threshold to 30%, however, preserves a significant fraction of the cooling effect, resulting in an ERF of -87 ± 6 mW m^{-2}. This represents the lowest loss of cooling among all regulation scenarios explored here (25 ± 17 mW m^{-2}). This demonstrates that a scenario specifically targeting the cloudy regions can be effective at reducing the loss of cooling resulting from the IMO2020 regulations.

3.2 Air quality impacts

Air quality impacts are presented in terms of ship-induced changes in the mean near-surface $PM_{2.5}$ concentrations in Fig. 3a. As expected, the PRE-IMO scenario produces the highest ship-induced $PM_{2.5}$ concentrations among all scenarios. In this scenario, ship emissions are responsible for an increase in the absolute mean $PM_{2.5}$ concentrations of about 1.5 μg m^{-3} in the 60 most populous coastal cities on the globe, reflecting the strong contribution of sulfur emissions from ships to particulate matter formation in coastal regions. Surface $PM_{2.5}$ mass concentrations are particularly high in the European (2.4 μg m^{-3}), Asian (2.8 μg m^{-3}) and African (1.9 μg m^{-3}) coastal cities. These values are especially notable for Europe, since they represent 2010

https://doi.org/10.5194/egusphere-2026-6471
Preprint. Discussion started: 16 November 2026
© Author(s) 2026. CC BY 4.0 License.

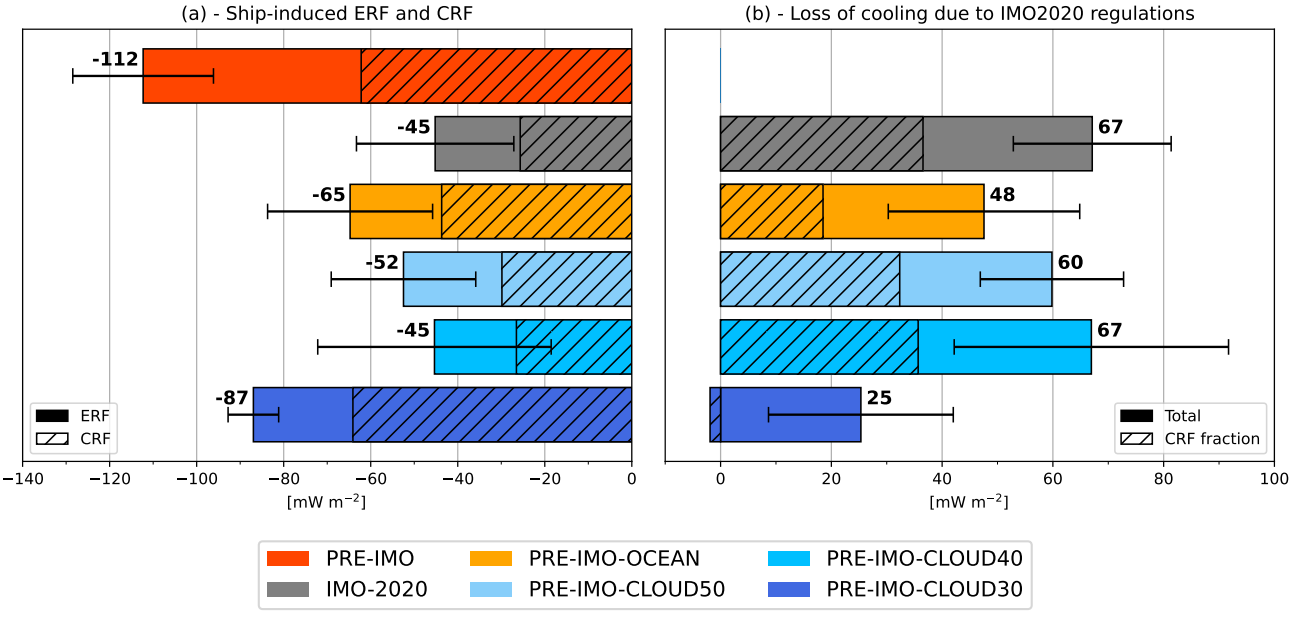


Figure 2. Ship-induced climate effects for the simulations performed in this study: a) effective radiative forcing (ERF) and cloud radiative forcing (CRF). b) Loss of cooling due to the IMO2020 regulations, calculated as the difference between the ERF (CRF) in each simulation and the ERF (CRF) in the PRE-IMO simulation. The numbers next to each bar represent the corresponding values in mW m^{-2}. The errorbars represent the 95% confidence intervals.

conditions of FSC, when ECAs were already enforced in the North Sea and in the Baltic Sea, with a maximum allowable FSC of 1% (see Fig. 1). Without these early measures, the ship-induced $PM_{2.5}$ concentrations would have been even higher. Regarding the global relative impact, shipping-induced PM2.5 mass concentrations represent 6.4% of total $PM_{2.5}$ concentrations under PRE-IMO conditions with particularly high relative values in Europe (9.8%) and Africa (7.9%), followed by Asia (6.3%), North America (5.1%), South America (2.8%) and Oceania (1.5%).

Ship-induced $PM_{2.5}$ concentrations are substantially reduced in the IMO-2020 scenario, with a global average decrease of 53% with respect to PRE-IMO conditions. This highlights the effectiveness of the sulfur regulations in mitigating air pollution from the shipping sector. A similar reduction is found for the PRE-IMO-OCEAN scenario, in which the IMO2020 regulations are applied only in coastal regions. This indicates that reducing sulfur emissions near densely populated coastal areas can be particularly effective in improving air quality. However, the magnitude of the reduction varies between continents. For instance, Asian coastal cities experience the largest decrease in $PM_{2.5}$ concentrations, from approximately 2.8 to 1.1 $\mu g\,m^{-3}$ (a reduction of 61%), and North American coastal cities from 0.8 to 0.2 $\mu g\,m^{-3}$ (75% reduction). In contrast, Europe shows a smaller reduction, from 2.4 to 1.3 $\mu g\,m^{-3}$ (46% reduction). The smaller response in Europe might be due to the early implementation of ECAs before 2010, which explains why the further improvements in air quality were smaller in Europe than in Asia and North America, where PRE-IMO $PM_{2.5}$ concentrations are higher. The same conclusions hold for the relative

https://doi.org/10.5194/egusphere-2026-6471
Preprint. Discussion started: 16 November 2026
© Author(s) 2026. CC BY 4.0 License.

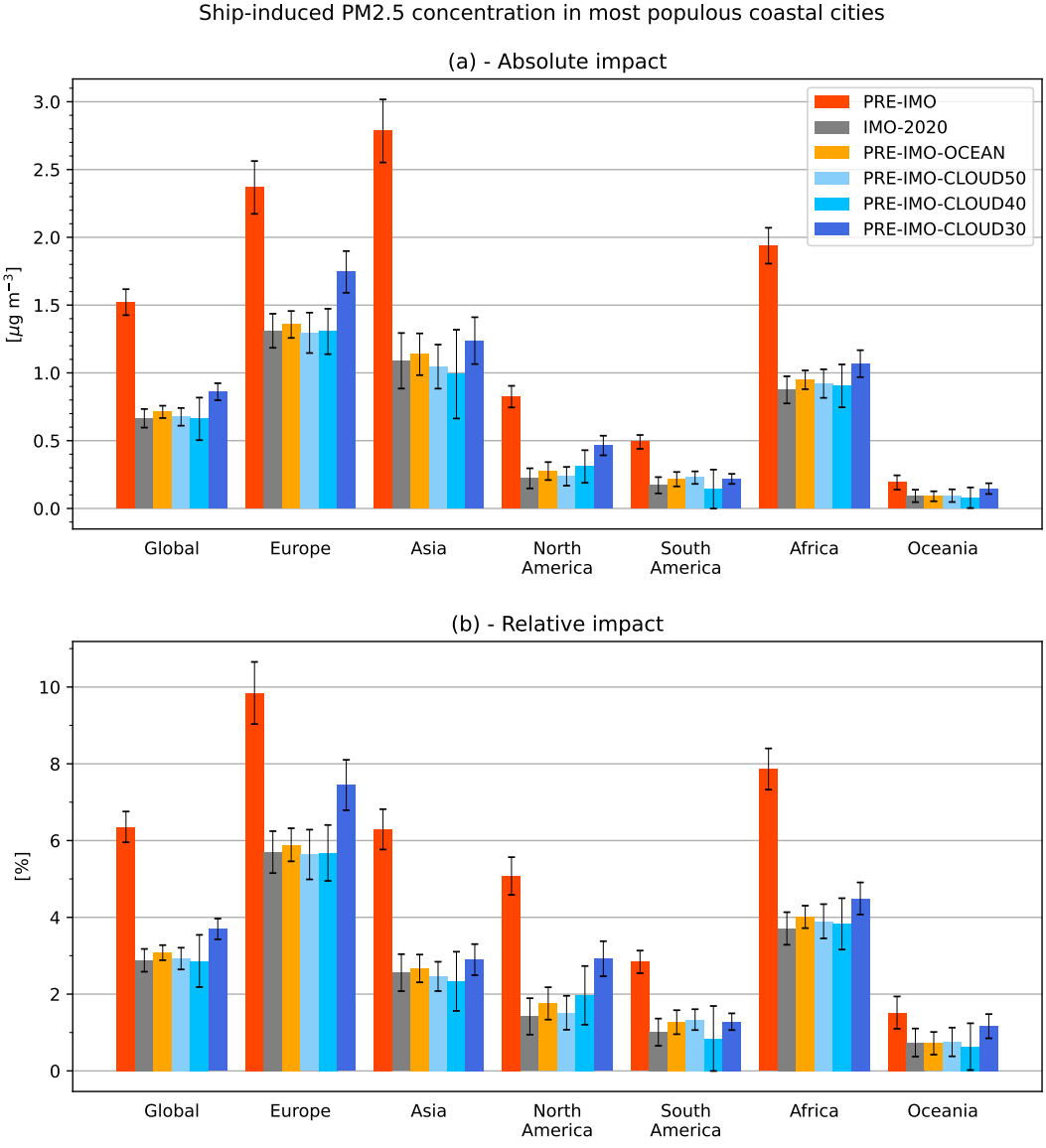


Figure 3. Absolute (a) and relative (b) ship-induced change in near-surface $PM_{2.5}$ concentration at the global level and in the 10 most populous coastal cities of each continent (see Fig. S6) for the six simulations performed in this study. The values are derived from multi-annual averages of the large-scale mean concentrations in the respective model grid-boxes. The errorbars indicate the 95% confidence interval.

impact of shipping to $PM_{2.5}$ concentrations. Under IMO-2020, the relative impact is reduced to 2.9% globally. A comparable reduction is found under the PRE-IMO-OCEAN scenario, where the impact would be 3.1%.

https://doi.org/10.5194/egusphere-2026-6471
Preprint. Discussion started: 16 November 2026
© Author(s) 2026. CC BY 4.0 License.

Ship-induced $PM_{2.5}$ concentrations in both the PRE-IMO-CLOUD50 and PRE-IMO-CLOUD40 scenarios are similar to those under IMO-2020 conditions. Thus, restricting the FSC in marine fuels in regions with extensive low-level clouds can largely preserve the air-quality benefits of the IMO2020 regulations. In contrast, the more extreme PRE-IMO-CLOUD30 scenario results in higher $PM_{2.5}$ concentrations than all other regulated scenarios, while still remaining significantly lower than for PRE-IMO conditions. Due to the geographical distribution of the low-level cloud cover (see Fig. S3), the ship-induced $PM_{2.5}$ concentrations increase in particular in Europe and North America, with respect to the IMO-2020 scenario.

4 Discussion

4.1 Comparison with previous studies

Figure 4 compares the loss of aerosol cooling in this study with values reported in previous studies that also investigated the impact of the IMO2020 regulations on the ship-induced ERF. The estimates for the loss of cooling span a wide range from approximately 27 to 500 mW m^{-2}, reflecting methodological differences between the studies. The estimate of the present study lies near the lower end of this range with a value of 67 mW m^{-2}. All model-based studies apply a perturbation approach, in which sulfur emissions from international shipping are reduced by approximately 80%, which represents the enforcement of the IMO2020 regulations. However, the resulting loss of cooling effects differ because of variations in emission inventories, model configurations, simulation lengths and representation of aerosol microphysics and cloud processes. While the majority of the studies, including this work, rely on simulations from a single model, other approaches include multi-model ensembles (Skeie et al., 2024), statistical methods (Diamond, 2023) and observational methods (Hansen et al., 2025).

Our results are most closely comparable with those by Sofiev et al. (2018) and Skeie et al. (2024). Sofiev et al. (2018) used the SILAM chemical transport model and AIS-based shipping emission inventories, projecting 2015 emissions to 2020, and found a loss of aerosol cooling of 71 mW m^{-2} in a scenario representing the enforcement of IMO-2020. Skeie et al. (2024) analyzed output from four global climate models (CESM2, ModelE MATRIX, ModelE OMA, NorESM2) and a chemistry transport model (OsloCTM3) and estimated the global loss of aerosol cooling relative to 2019 shipping emissions. For each model, two ensemble members were run with simulation lengths ranging from 50 to 200 years in order to improve the signal-to-noise ratio. The model-specific mean loss of coolings range from 60 to 90 mW m^{-2}, with a multi-model mean of 73 mW m^{-2}. This is close to our estimate. Skeie et al. (2024) also assumed a sulfur reduction of 8.7 Tg but used the CEDS emission inventory (Hoesly et al., 2018). Among the four models, CESM2 estimated the largest loss of aerosol-induced cooling, with a mean of 90 mW m^{-2} across the two ensemble simulations.

Hausfather and Forster (2023) estimated that the global sulfur emission reduction of 8.5 Tg caused a loss of cooling of 79 mW m^{-2}, which is also close to our result. In contrast, Gettelman et al. (2024), using CESM2, reported a higher global loss of aerosol cooling of 120 ± 30 mW m^{-2}. They used a shorter 12-year simulation period compared to Skeie et al. (2024), which may lead to a shorter sampling time of internal variability and may therefore affect the estimated forcing (both overestimation or underestimation is possible). Yoshioka et al. (2024) also reported a higher global mean loss of cooling of 130 ± 20 mW m^{-2} using UKESM with a simulation period of 9 years. Yuan et al. (2022) estimated a substantially larger loss of aerosol cooling

https://doi.org/10.5194/egusphere-2026-6471
Preprint. Discussion started: 16 November 2026
© Author(s) 2026. CC BY 4.0 License.

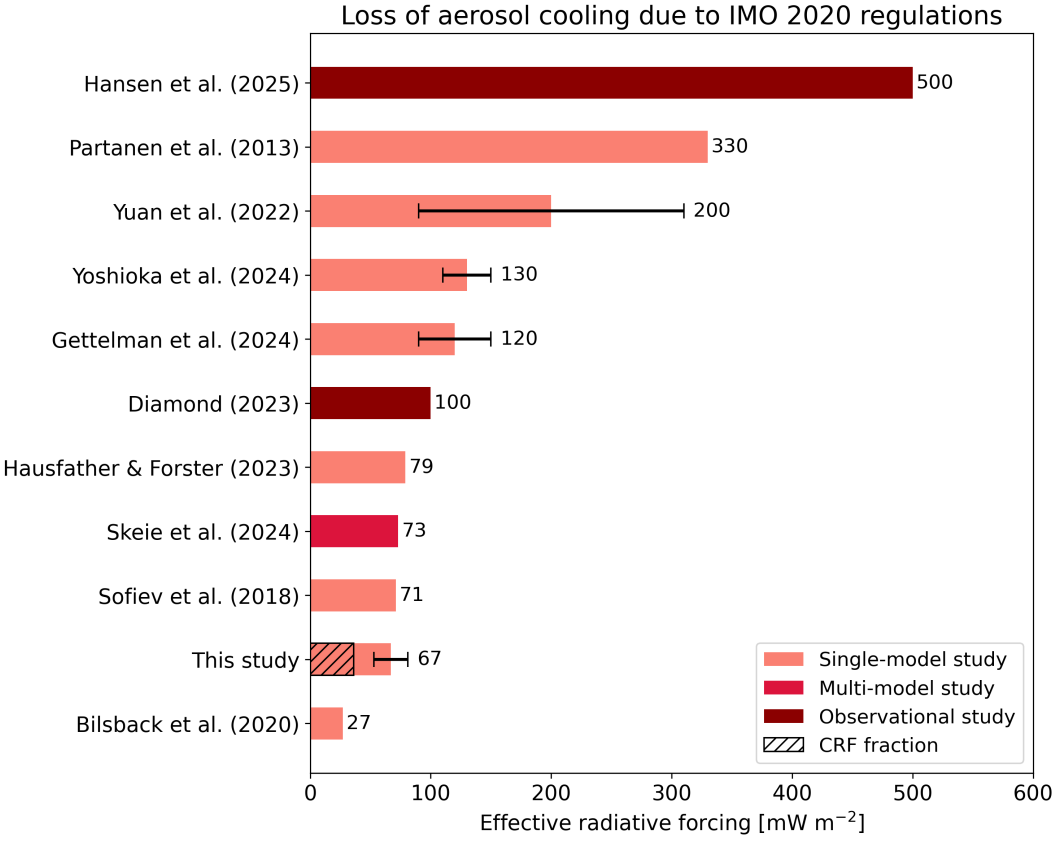


Figure 4. Overview of the literature results on the loss of aerosol cooling attributable to the IMO2020 regulations, compared with the results of this study. The numbers next to each bar represent the corresponding values in mW m^{-2}.

of 200 mW m^{-2} by combining satellite observations from MODIS and CERES with the NASA GEOS-GOCART chemical transport model. Their estimate, however, is averaged over the global ocean rather than over the entire Earth: since open-ocean regions often include areas of high cloud susceptibility to aerosol perturbations, this approach yields a larger ERF losses than global-mean calculations. However, their shipping-induced change in cloud droplet number is small compared to natural background variability, which may contribute to the large uncertainty of $\pm$110 mW m^{-2}.

An even larger estimate was reported by Partanen et al. (2013), who found a loss of aerosol cooling of 330 mW m^{-2}. Their study used a larger reduction in SO_x emissions (11.1 Tg) and used baseline data from the ACCMIP inventory, implemented within the ECHAM-HAMMOZ climate model. A limit of 0.1% FSC within 200 nautical miles of coastlines and 0.5% FSC elsewhere was applied in their scenario. This differs from the actual IMO2020 regulations, which consider a 0.1% limit only in the ECAs and a 0.5% limit outside ECAs, and may enhance the estimated loss of cooling because coastal areas are exposed to dense ship traffic. Moreover, Partanen et al. (2013) assumed a median diameter of 44 nm for emitted sulfate particles. In contrast, the MADE3 aerosol scheme used in this work assumes that 10% of the shipping mass emissions is released into the

https://doi.org/10.5194/egusphere-2026-6471
Preprint. Discussion started: 16 November 2026
© Author(s) 2026. CC BY 4.0 License.

Aitken mode with a median diameter of 70 nm, while 90% into the accumulation mode with a median diameter of 260 nm (Kaiser et al., 2019). This represents a more aged particle population and implicitly accounts for unresolved microphysical processes in ship plumes (Petzold et al., 2008; Righi et al., 2013). Smaller exhaust particles imply higher particle number emissions for the same emitted mass and may therefore enhance the CCN perturbation and the simulated aerosol-cloud response. This may partly explain our comparatively small ERF estimate. Bilsback et al. (2020) reported one of the smallest estimates, with a loss of aerosol cooling of 27 mW m^{-2} using GEOS-Chem-TOMAS. They applied an 85% reduction in SO_x emissions, from 8.98 to 1.35 Tg, corresponding to a reduction of 7.63 Tg. This emission reduction is slightly smaller than that considered by Skeie et al. (2024) and in our study, which may contribute to their smaller estimate of the loss of the cooling.

Diamond (2023) applied a statistical method to assess changes in cloud properties in the southeastern Atlantic shipping corridor. Their study found a local loss of cooling from aerosol-cloud interactions of the order of 1000 mW m^{-2}, corresponding to a global-mean estimate of about 100 mW m^{-2}. Hansen et al. (2025), based on observed changes in absorbed solar radiation, suggested that the reduction in ship-induced aerosol particles after the IMO2020 regulations could have caused a loss of aerosol cooling of about 500 mW m^{-2}. This value is substantially larger than most model-based estimates and should therefore be interpreted in the context of the observational methods and assumptions used in that study.

Overall, the wide spread of published estimates shows that the loss of aerosol cooling from the IMO2020 regulations is highly sensitive to methodological choices. Notably, the upper end of the estimated loss of aerosol coolings (up to 500 mW m^{-2}) is comparable to, and in some cases exceeds, earlier estimates of the total shipping-induced aerosol cooling (-146 to -600 mW m^{-2}). This comparison highlights that the magnitude of the estimated loss needs to be considered relative to the corresponding baseline shipping-induced aerosol ERF, which itself varies substantially among studies. Differences in emission inventories, i.e. emission totals and spatial distribution, model resolution, assumptions on the size distribution of the ship-emitted particles and resulting particle number emissions can all influence the changes in CCN and the resulting ERF. As shown by Lauer et al. (2007), both the magnitude of emissions and their location relative to clouds are very important to the ERF response. Despite the large quantitative spread, all studies consistently indicate that the IMO2020 regulation on FSC reduced the net negative ERF of shipping emissions, thereby weakening the aerosol-induced cooling effect from international shipping.

4.2 Emission regulation scenarios

A key result of our work is that a substantial loss of aerosol cooling already appears when the IMO2020 regulations are only applied to coastal regions, while ships operating in the open ocean continue to use PRE-IMO high sulfur fuels (PRE-IMO-OCEAN scenario). This scenario leads to a global mean loss of aerosol cooling of 48 ± 17 mW m^{-2}. The dominant contribution of coastal sulfur reductions can be explained by two factors. First, coastal regions include the bulk of ship traffic, i.e. 82% of global shipping activity and associated CO_2 emissions, as well as 86% of global SO_x emissions, due to the high traffic density near coasts (see Table 1). In contrast, only 18% of shipping activity occurs in open ocean regions. Second, low-level cloud regimes, such as marine stratocumulus clouds, occur frequently in both coastal and open ocean regions and are highly susceptible to aerosol perturbations. In the model, applying sulfur limits only in coastal regions weakens the CRF by about 18 mW m^{-2}, corresponding to approximately 40%. However, the CRF estimates carry substantial uncertainties, making

https://doi.org/10.5194/egusphere-2026-6471
Preprint. Discussion started: 16 November 2026
© Author(s) 2026. CC BY 4.0 License.

a precise attribution of the response difficult. Overall, coastal sulfur reductions alone account for approximately a loss of 42% of the PRE-IMO ERF. Therefore, the largest loss of aerosol-induced cooling is found when FSC limits are enforced globally, affecting both coastal and open ocean regions.

The three scenarios focusing on low-level clouds further demonstrate that the assumed cloud-cover fraction thresholds strongly influence the resulting loss of aerosol cooling. The largest loss of aerosol-induced cooling is found for the PRE-IMO-CLOUD40 and PRE-IMO-CLOUD50 scenarios. The reason is that these thresholds of 40% and 50% for the average low-level cloud amount restrict the use of high-sulfur fuels to a comparatively small fraction of the ocean (Fig. S3). As a result, large oceanic regions remain subject to the IMO-2020 sulfur limits, which leads to a substantial reduction in aerosol-induced cooling. In contrast, the PRE-IMO-CLOUD30 scenario exhibits the smallest loss of aerosol cooling and therefore preserves the largest fraction of the PRE-IMO cooling effect. This can be explained by the much larger spatial extent of regions with an average low-level cloud cover exceeding 30%. Since a large fraction of the ocean satisfies this lower threshold according to the 20-year mean of satellite cloud data, PRE-IMO FSC is retained over large oceanic areas. Consequently, sulfur emissions remain higher over a large part of the ocean. Aerosol-cloud interactions and the associated marine cloud brightening effect can persist more strongly than in other scenarios. At the same time, the large ocean areas make this scenario quite unfeasible, as it would imply returning to PRE-IMO regulations in several regions of the globe, including some coastal areas, thus compromising part of the air quality benefits achieved by the FSC regulations. However, it is important to note, that the cloud cover masks used here are based on low-level cloud-cover data from satellite measurements and are not identical to the cloud-cover distribution simulated by EMAC. Although the mask determines where pre-IMO conditions are applied, the ERF response is calculated by EMAC and therefore depends on the modelled cloud cover and ACIs. Righi et al. (2020) showed that EMAC captures the large-scale pattern of total cloud cover well compared to ESA Cloud_cci data, but also exhibits regional biases. EMAC slightly overestimates total cloud cover in the tropics and underestimates cloud cover in stratocumulus regions off the western coasts of South America, Africa and Australia. These biases could affect the ERF response, especially for the more restrictive PRE-IMO-CLOUD40 and PRE-IMO-CLOUD50 masks. For PRE-IMO-CLOUD30, the effect on the spatial selection is likely smaller, because large parts of the ocean remain anyway under pre-IMO conditions. For PRE-IMO-CLOUD50, however, an underestimation of marine stratocumulus clouds in EMAC could weaken the simulated ACIs in regions where shipping aerosols are expected to be most effective, potentially leading to an underestimation of the negative ERF.

4.3 Air quality impacts and trade-off with climate effects

Our results in Fig. 3 show that the IMO2020 regulations significantly improved air quality in coastal regions. In the absence of these regulations, ship-induced $PM_{2.5}$ mass concentrations in the world's most populous coastal cities would be more than twice as high. The reductions are particularly pronounced in Asian, African and European coastal cities. This reflects the high density of shipping activity near coastlines and along major shipping corridors, such as the Mediterranean Sea, the English Channel and in Southeast Asia. For European coastal cities, our result for the mean $PM_{2.5}$ contribution from shipping emissions under PRE-IMO conditions is broadly consistent with Partanen et al. (2013), who estimated maximum shipping-induced $PM_{2.5}$ concentrations of 2 $\mu g\,m^{-3}$ for western Europe's coastal regions.

https://doi.org/10.5194/egusphere-2026-6471
Preprint. Discussion started: 16 November 2026
© Author(s) 2026. CC BY 4.0 License.

Since the primary aim of the IMO2020 regulations was to improve air quality, the resulting loss of aerosol cooling constitutes an unintended side effect. This highlights the trade-off faced by policymakers: reducing sulfur emissions from shipping considerably improves air quality, but at the same time weakens the negative ERF from shipping aerosols. This trade-off is not only specific to shipping, but it represents a general challenge in managing the mitigation of air-pollution, although the high FSC of shipping fuels compared to other transport sectors makes shipping a sensible target for such mitigation measures.

Figure 5 illustrates this trade-off between climate and air quality for the shipping sector. The x-axis shows the global-mean ship-induced $PM_{2.5}$ concentrations in the most populous coastal cities, while the y-axis displays the corresponding ship-induced ERF (cooling effect). Scenarios with reduced SO_x emissions from ships lead to lower $PM_{2.5}$ concentrations and therefore improved air quality, but also to a decrease in aerosol-induced cooling (top-right portion of the diagram). When limiting SO_x emissions in coastal regions (PRE-IMO-OCEAN scenario), substantial air-quality benefits are achieved at the cost of a 42% loss of cooling relative to PRE-IMO.

From the perspective of addressing air pollution and at the same time trying to maintain the cooling, an ideal outcome would combine minimal $PM_{2.5}$ concentrations with maximal aerosol-induced cooling. However, the scenarios investigated in this work suggest that such an optimum is hard to achieve: Either air quality is improved while reducing the cooling effect or the cooling is retained at the cost of continued air pollution. The scenario that comes closest to this balance is PRE-IMO-CLOUD30, which preserves the largest fraction of aerosol-induced cooling (78%) while still reducing $PM_{2.5}$ concentrations relative to PRE-IMO conditions (43%). However, the 30% cloud cover threshold is satisfied in large parts of the oceanic regions according to the satellite data. From a regulatory perspective, such a threshold may therefore be difficult to justify, as it would permit the use of high FSC over extensive areas and thus provide only a weak spatial restriction. In addition, the cloud-cover threshold used in this study is based on a 20-year climatological mean and therefore does not necessarily represent the actual low-level cloud cover in the model. Seasonal variability may cause deviations from this mean state. This limits the feasibility of this scenario in the real world.

4.4 Uncertainties

Estimates of the shipping ERF due to IMO2020 regulations is subject to substantial uncertainty. In this study, the uncertainty associated with the ERF and loss of cooling values is expressed as a 95% confidence interval, calculated from the interannual variability of the 10-year EMAC simulations. A major contribution to this uncertainty arises from aerosol-cloud interactions, which account for approximately 50-70% of the total net cooling effect but exhibit strong interannual variability. Additional uncertainty is related to emission estimates and to the representation of the atmospheric sulfur cycle in the model. The response of clouds to aerosol emission changes is also highly inherently non-linear. According to Twomey (1977) and Carslaw et al. (2013), the sensitivity of cloud albedo to aerosol changes decreases under more polluted baseline conditions: in clean environments, small increases in aerosols can lead to strong cloud-albedo responses, whereas in already polluted environments the effect saturates and becomes weak. Because the IMO2020 scenario shifts the system from a polluted to a cleaner regime, the non-linear response of the aerosol-cloud system could explain why an 80% reduction in SO_x emissions results in a smaller, approximately 60% reduction in aerosol-induced cooling rather than a proportional change in ERF. Hence, the model repre-

https://doi.org/10.5194/egusphere-2026-6471
Preprint. Discussion started: 16 November 2026
© Author(s) 2026. CC BY 4.0 License.

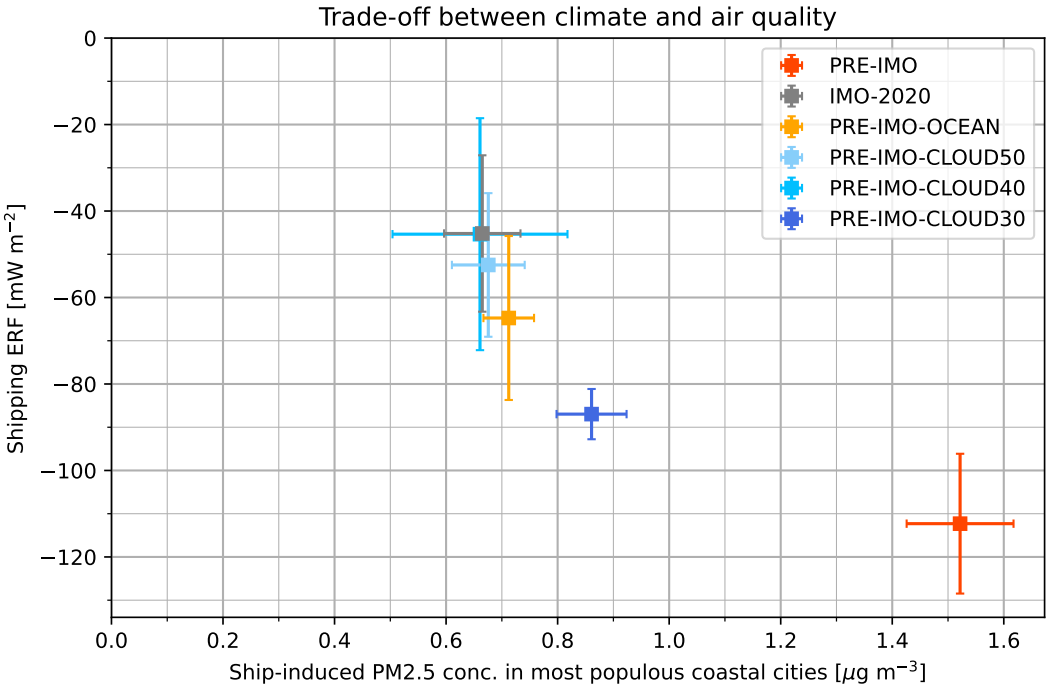


Figure 5. Trade-off between $PM_{2.5}$ concentrations and the net ERF resulting from ship emissions under different emission scenarios. Each point represents the results regarding air quality effects and radiative effects from shipping emissions for each scenario analyzed in this study. The lower left portion of the plot represent the ideal situation limiting both the detrimental effects on air quality and the loss of cooling from ship emissions. The errorbars represent the 95% confidence intervals.

sentation of the aerosol background concentrations and of the cloud mean state is another relevant source of uncertainties. Finally, a further limitation of the present simulations is that they do not distinguish between different compliance strategies, such as the use of low-sulfur fuels and exhaust gas cleaning systems. These strategies may affect particle size distributions and, consequently, cloud microphysical responses (Escusa dos Santos et al., 2025). Instead, our model assumes the same particle number size distribution across all simulations due to limited data availability on the size distributions of emitted particles for different FSC. Moreover, a global model is not capable of resolving the (non-linear) plume processes, therefore it would be difficult to test different size distributions for the particles emitted by different fuels, since these are usually measured in the fresh exhaust, which is not representative for large scale effects addressed here.

5 Conclusions

Recent regulations introduced by the International Maritime Organization (IMO2020) reduced the sulfur content in ship fuels by approximately 80%. These regulations aimed to improve air quality and thus protect human health and the environment,

https://doi.org/10.5194/egusphere-2026-6471
Preprint. Discussion started: 16 November 2026
© Author(s) 2026. CC BY 4.0 License.

especially in coastal regions where air quality is strongly affected by ship traffic. However, the reduction of sulfur emissions has also decreased the radiative cooling effect of aerosol particles, thereby contributing to a net radiative warming of the climate system. In this study, we quantified a global-mean loss of cooling due to the IMO2020 regulations of 67 ± 14 mW m^{-2}, corresponding to 60% of the shipping ERF. Compared to previous estimates from other studies, our result is in good agreement with the multi-model mean reported by Skeie et al. (2024) and the single-model study result reported by Sofiev et al. (2018), although other studies reported larger values. Such a large spread in the values reported in literature can partly be explained by differences in methodological approaches, underlying assumptions, and the overall uncertainty associated with aerosol-cloud interactions. In terms of air quality impacts, we found that ship-induced near-surface $PM_{2.5}$ concentrations in the most populous coastal cities of the world decreased by 57% due to IMO2020 regulations. We also investigated hypothetical regulation scenarios and found that especially enforcing a 0.5%-limit only in coastal regions, while keeping pre-IMO sulfur limits over the open ocean, is particularly effective at improving air quality in coastal areas, since emissions in these regions have the largest impact on coastal pollution exposure. However, the loss of aerosol-induced cooling remains high, at 48 ± 17 mW m^{-2} (43% of the shipping ERF). This indicates that under this scenario, improving air quality while maintaining the cooling effect of ship emissions is not achievable. The only scenario that comes close to an ideal trade-off between air quality benefits and a limited loss of cooling considers pre-IMO sulfur limits in regions with persistent low-level cloud cover above 30% on a climatological mean basis. Given the large spatial extent of such regions, covering also several coastal areas, this scenario is considered rather suboptimal. In addition, average $PM_{2.5}$ concentrations in the coastal cities are reduced by only 43% instead of 57% as in IMO-2020.

For policymakers, the trade-off between climate protection and air quality improvements remains an ongoing debate and the shipping sector is just one prominent example of this trade-off. The ERF from shipping has been shown to exhibit strong regional differences. Gettelman et al. (2024) found that the net ERF is heavily centered in the Northern Hemisphere due to higher shipping activity, resulting in regional warming effects that are significantly larger than the global average, with possible impacts on atmospheric circulation and dynamics. This is supported by the ship-track reduction studies conducted by Yuan et al. (2022) and Watson-Parris et al. (2022), which highlighted the spatial correlation between aerosol-cloud interactions and shipping lanes. Partanen et al. (2013) identified the strongest aerosol-induced cooling over the stratocumulus regions of the North Pacific, where low-level clouds that are highly susceptible to aerosol perturbations coincide with high ship emissions along major trade routes. These findings suggest that policymakers might consider implementing different sulfur regulations for different regions rather than enforcing a global approach outside the coastal areas. For instance, in oceanic stratocumulus regions where the aerosol-cooling effect is high, it may be possible to apply less stringent fuel sulfur limits without significantly affecting air quality. Moreover, higher-resolution model simulations could be used to explore whether low-sulfur emission control areas could be restricted to narrower coastal bands, thereby preserving air-quality benefits while further reducing the loss of aerosol-induced cooling. Future research could also focus on the long-range transport of aerosol particles from shipping to assess the extent to which emissions from open ocean regions might still affect air quality in distant coastal or inland areas. Further investigations should also focus on how low sulfur fuels versus the use of conventional fuels in combination with wet scrubbers to remove sulfur from the exhaust affect the emitted particle number and size distribution. This would allow to achieve

https://doi.org/10.5194/egusphere-2026-6471
Preprint. Discussion started: 16 November 2026
© Author(s) 2026. CC BY 4.0 License.

a better understanding of the consequences of technical implementation of sulfur reduction strategies. Escusa dos Santos et al. (2025) showed that the particle exhaust of scrubbers is subject to large variability and largely depends on the fuel type. Recently, Zhang et al. (2024) identified a potential unintended side effect of the IMO2020 regulations: the reduction of SO_x and particle emissions causes an increase of NMVOC, which are precursors to tropospheric ozone and secondary organic aerosol formation, both being detrimental to air quality. Also, Kokkola et al. (2026) show that IMO-compliant fuels such as low-sulfur heavy fuel oil (LS-HFO) and marine gas oil (MGO) emit BC-rich particles and may even produce a more positive radiative effect than conventional high-sulfur HFO. This highlights the complexity of atmospheric responses to emission controls and the continued need to assess the significance of such side effects in a more comprehensive manner. The IMO2020 regulations provided an opportunity for real-world experiments on geoengineering strategies such as marine cloud brightening, as the relatively sudden reduction of ship sulfur emissions allows to investigate how sensitive low marine clouds are to changes in aerosol concentrations. In the near future, alternative fuels such as biofuels, ammonia, liquified natural gas, and methane are expected to gain more importance, as the shipping sector faces the challenges of defossilisation and net-zero emission targets, and their effects on both air quality and climate would need to be assessed in detail, considering GHGs and SLCFs and the climate-air quality trade-offs in a comprehensive way.

Data availability. The simulation data described in this work will be made available with the final version of the manuscript.

Author contributions. LI performed the model simulations, analyzed the output and wrote the paper; MR and AS conceived the study and contributed to the analysis and the writing; JH and AL contributed to discussions of the results and helped with the observational data. All authors contributed to the text.

Competing interests. The authors declare no competing interests.

Acknowledgements. We are grateful to Qiang Li (DLR, Germany) for his insightful comments on an earlier version of this manuscript. The model simulations and data analysis for this work used the resources of the Deutsches Klimarechenzentrum (DKRZ) granted by its Scientific Steering Committee WLA) under project ID bb1393.

Financial support. This study was supported by the DLR transport research program (MoDa project).

https://doi.org/10.5194/egusphere-2026-6471
Preprint. Discussion started: 16 November 2026
© Author(s) 2026. CC BY 4.0 License.

References

Albrecht, B. A.: Aerosols, Cloud Microphysics, and Fractional Cloudiness, Science, 245, 1227–1230, https://doi.org/10.1126/science.245.4923.1227, 1989.

Bilsback, K. R., Kerry, D., Croft, B., Ford, B., Jathar, S. H., Carter, E., Martin, R. V., and Pierce, J. R.: Beyond SO_x reductions from shipping: assessing the impact of NOx and carbonaceous-particle controls on human health and climate, Environ. Res. Lett., 15, 124 046, https://doi.org/10.1088/1748-9326/abc718, 2020.

Buhaug, , Corbett, J. J., Endresen, , Eyring, V., Faber, J., Hanayama, S., Lee, D. S., Lee, D., Lindstad, H., Markowska, A. Z., Mjelde, A., Nelissen, D., Nilsen, J., Pålsson, C., Winebrake, J. J., Wu, W., and Yoshida, K.: Second IMO GHG Study 2009, Tech. rep., International Maritime Organization (IMO), London, UK, 2009.

Carslaw, K. S., Lee, L. A., Reddington, C. L., Pringle, K. J., Rap, A., Forster, P. M., Mann, G. W., Spracklen, D. V., Woodhouse, M. T., Regayre, L. A., and Pierce, J. R.: Large contribution of natural aerosols to uncertainty in indirect forcing, Nature, 503, 67–71, https://doi.org/10.1038/nature12674, 2013.

Chen, T., Rossow, W. B., and Zhang, Y.: Radiative Effects of Cloud-Type Variations, J. Climate, 13, 264–286, https://doi.org/10.1175/1520-0442(2000)013<0264:reoctv>2.0.co;2, 2000.

Copernicus Atmosphere Monitoring Service: CAMS global biomass burning emissions based on fire radiative power (GFAS), Copernicus Atmosphere Monitoring Service (CAMS) Atmosphere Data Store, https://doi.org/10.24381/a05253c7, last access: 24/03/2026, 2022.

Corbett, J. J., Winebrake, J. J., Green, E. H., Kasibhatla, P., Eyring, V., and Lauer, A.: Mortality from Ship Emissions: A Global Assessment, Environ. Sci. Technol., 41, 8512–8518, https://doi.org/10.1021/es071686z, 2007.

Diamond, M. S.: Detection of large-scale cloud microphysical changes within a major shipping corridor after implementation of the International Maritime Organization 2020 fuel sulfur regulations, Atmos. Chem. Phys., 23, 8259–8269, https://doi.org/10.5194/acp-23-8259-2023, 2023.

Dietmüller, S., Jöckel, P., Tost, H., Kunze, M., Gellhorn, C., Brinkop, S., Frömming, C., Ponater, M., Steil, B., Lauer, A., and Hendricks, J.: A new radiation infrastructure for the Modular Earth Submodel System (MESSy, based on version 2.51), Geosci. Model Dev., 9, 2209–2222, https://doi.org/10.5194/gmd-9-2209-2016, 2016.

Escusa dos Santos, L. F., Frostenberg, H. C., Baró Pérez, A., Ekman, A. M. L., Ickes, L., and Thomson, E. S.: Potential impacts of marine fuel regulations on an Arctic stratocumulus case and its radiative response, Atmos. Chem. Phys., 25, 119–142, https://doi.org/10.5194/acp-25-119-2025, 2025.

Eyring, V., Isaksen, I. S., Berntsen, T., Collins, W. J., Corbett, J. J., Endresen, O., Grainger, R. G., Moldanova, J., Schlager, H., and Stevenson, D. S.: Transport impacts on atmosphere and climate: Shipping, Atmos. Environ., 44, 4735–4771, https://doi.org/10.1016/j.atmosenv.2009.04.059, 2010.

Faber, J., Hanayama, S., Zhang, S., Pereda, P., Comer, B., Hauerhof, E., Schim van der Loeff, W., Smith, T., Zhang, Y., Kosaka, H., Adachi, M., Bonello, J.-M., Galbraith, C., Gong, Z., Hirata, K., Hummels, D., Kleijn, A., Lee, D. S., Liu, Y., Lucchesi, A., Mao, X., Muraoka, E., Osipova, L., Qian, H., Rutherford, D., Suárez de la Fuente, S., Yuan, H., Velandia Perico, C., Wu, L., Sun, D., Yoo, D.-H., and Xing, H.: Fourth IMO GHG Study 2020, Tech. rep., International Maritime Organization, London, https://www.imo.org/en/OurWork/Environment/Pages/Fourth-IMO-GHG-Study-2020.aspx, 2021.

Flanders Marine Institute: Maritime Boundaries Geodatabase: Maritime Boundaries and Exclusive Economic Zones (200NM), version 12, Available online at https://www.marineregions.org/, https://doi.org/10.14284/632, last access: 24/03/2026, 2023.

https://doi.org/10.5194/egusphere-2026-6471
Preprint. Discussion started: 16 November 2026
© Author(s) 2026. CC BY 4.0 License.



Gettelman, A., Christensen, M. W., Diamond, M. S., Gryspeerdt, E., Manshausen, P., Stier, P., Watson-Parris, D., Yang, M., Yoshioka, M., and Yuan, T.: Has Reducing Ship Emissions Brought Forward Global Warming?, Geophys. Res. Lett., 51, https://doi.org/10.1029/2024gl109077, 2024.

Gidden, M. J., Riahi, K., Smith, S. J., Fujimori, S., Luderer, G., Kriegler, E., van Vuuren, D. P., van den Berg, M., Feng, L., Klein, D., Calvin, K., Doelman, J. C., Frank, S., Fricko, O., Harmsen, M., Hasegawa, T., Havlik, P., Hilaire, J., Hoesly, R., Horing, J., Popp, A., Stehfest, E., and Takahashi, K.: Global emissions pathways under different socioeconomic scenarios for use in CMIP6: a dataset of harmonized emissions trajectories through the end of the century, Geosci. Model Dev., 12, 1443–1475, https://doi.org/10.5194/gmd-12-1443-2019, 2019.

Hansen, J. E., Kharecha, P., Sato, M., Tselioudis, G., Kelly, J., Bauer, S. E., Ruedy, R., Jeong, E., Jin, Q., Rignot, E., Velicogna, I., Schoeberl, M. R., von Schuckmann, K., Amponsem, J., Cao, J., Keskinen, A., Li, J., and Pokela, A.: Global Warming Has Accelerated: Are the United Nations and the Public Well-Informed?, Environ.: Sci. Policy Sustainable Dev, 67, 6–44, https://doi.org/10.1080/00139157.2025.2434494, 2025.

Hausfather, Z. and Forster, P.: Analysis: How low-sulphur shipping rules are affecting global warming, https://www.carbonbrief.org/analysis-how-low-sulphur-shipping-rules-are-affecting-global-warming/, 2023.

Hendricks, J., Righi, M., Brinkop, S., Dahlmann, K., Mertens, M., Beer, C. G., Grewe, V., Kaiser, J. C., and Ponater, M.: Large present-day and future climate forcing due to non-CO2 emissions from global transport, npj Clim. Atmos. Sci., 9, https://doi.org/10.1038/s41612-026-01383-y, 2026.

Hersbach, H., Bell, B., Berrisford, P., Hirahara, S., Horányi, A., Muñoz-Sabater, J., Nicolas, J., Peubey, C., Radu, R., Schepers, D., Simmons, A., Soci, C., Abdalla, S., Abellan, X., Balsamo, G., Bechtold, P., Biavati, G., Bidlot, J., Bonavita, M., De Chiara, G., Dahlgren, P., Dee, D., Diamantakis, M., Dragani, R., Flemming, J., Forbes, R., Fuentes, M., Geer, A., Haimberger, L., Healy, S., Hogan, R. J., Hólm, E., Janisková, M., Keeley, S., Laloyaux, P., Lopez, P., Lupu, C., Radnoti, G., de Rosnay, P., Rozum, I., Vamborg, F., Villaume, S., and Thépaut, J.: The ERA5 global reanalysis, Quart. J. Roy. Meteorol. Soc., 146, 1999–2049, https://doi.org/10.1002/qj.3803, 2020.

Hoesly, R. M., Smith, S. J., Feng, L., Klimont, Z., Janssens-Maenhout, G., Pitkanen, T., Seibert, J. J., Vu, L., Andres, R. J., Bolt, R. M., Bond, T. C., Dawidowski, L., Kholod, N., ichi Kurokawa, J., Li, M., Liu, L., Lu, Z., Moura, M. C. P., O'Rourke, P. R., and Zhang, Q.: Historical (1750–2014) anthropogenic emissions of reactive gases and aerosols from the Community Emissions Data System (CEDS), Geosci. Model Dev., 11, 369–408, https://doi.org/10.5194/gmd-11-369-2018, 2018.

International Maritime Organization: Amendments to the Annex of the Protocol of 1997 to Amend the International Convention for the Prevention of Pollution from Ships, 1973, as Modified by the Protocol of 1978 Relating Thereto: Amendments to MARPOL Annex VI, Resolution MEPC.392(82), International Maritime Organization, https://wwwcdn.imo.org/localresources/en/OurWork/Environment/Documents/MEPC.392(82).pdf, last access: 2 September 2026, 2024.

Jaramillo, P., Kahn Ribeiro, S., Newman, P., Dhar, S., Diemuodeke, O. E., Kajino, T., Lee, D. S., Nugroho, S. B., Ou, X., Hammer Strømman, A., and Whitehead, J.: Transport, in: Climate Change 2022: Mitigation of Climate Change. Contribution of Working Group III to the Sixth Assessment Report of the Intergovernmental Panel on Climate Change, edited by Shukla, P. R., Skea, J., Slade, R., Al Khourdajie, A., van Diemen, R., McCollum, D., Pathak, M., Some, S., Vyas, P., Fradera, R., Belkacemi, M., Hasija, A., Lisboa, G., Luz, S., and Malley, J., Cambridge University Press, Cambridge, UK and New York, NY, USA, https://doi.org/10.1017/9781009157926.012, 2022.

Jöckel, P., Kerkweg, A., Pozzer, A., Sander, R., Tost, H., Riede, H., Baumgaertner, A., Gromov, S., and Kern, B.: Development cycle 2 of the Modular Earth Submodel System (MESSy2), Geosci. Model Dev., 3, 717–752, https://doi.org/10.5194/gmd-3-717-2010, 2010.

https://doi.org/10.5194/egusphere-2026-6471
Preprint. Discussion started: 16 November 2026
© Author(s) 2026. CC BY 4.0 License.



Jöckel, P., Tost, H., Pozzer, A., Kunze, M., Kirner, O., Brenninkmeijer, C. A. M., Brinkop, S., Cai, D. S., Dyroff, C., Eckstein, J., Frank, F., Garny, H., Gottschaldt, K.-D., Graf, P., Grewe, V., Kerkweg, A., Kern, B., Matthes, S., Mertens, M., Meul, S., Neumaier, M., Nützel, M., Oberländer-Hayn, S., Ruhnke, R., Runde, T., Sander, R., Scharffe, D., and Zahn, A.: Earth System Chemistry integrated Modelling (ESCiMo) with the Modular Earth Submodel System (MESSy) version 2.51, Geosci. Model Dev., 9, 1153–1200, https://doi.org/10.5194/gmd-9-1153-2016, 2016.

Johansson, L., Jalkanen, J.-P., and Kukkonen, J.: Global assessment of shipping emissions in 2015 on a high spatial and temporal resolution, Atmos. Environ., 167, 403–415, https://doi.org/10.1016/j.atmosenv.2017.08.042, 2017.

Kaiser, J. C., Hendricks, J., Righi, M., Riemer, N., Zaveri, R. A., Metzger, S., and Aquila, V.: The MESSy aerosol submodel MADE3 (v2.0b): description and a box model test, Geosci. Model Dev., 7, 1137–1157, https://doi.org/10.5194/gmd-7-1137-2014, 2014.

Kaiser, J. C., Hendricks, J., Righi, M., Jöckel, P., Tost, H., Kandler, K., Weinzierl, B., Sauer, D., Heimerl, K., Schwarz, J. P., Perring, A. E., and Popp, T.: Global aerosol modeling with MADE3 (v3.0) in EMAC (based on v2.53): model description and evaluation, Geosci. Model Dev., 12, 541–579, https://doi.org/10.5194/gmd-12-541-2019, 2019.

Kokkola, T., Sipkens, T. A., Paul, A., Shukla, D., Ihalainen, M., Das, A., Scott, J., Passig, J., Kalamašnikovs, A., Etzien, U., Fang, Z., Mikkonen, S., Hartikainen, A., Luostari, V., Mukherjee, A., Czech, H., Sklorz, M., Buchholz, B., Streibel, T., Hohaus, T., Rudich, Y., Øvrevik, J., Zimmermann, R., Corbin, J. C., and Sippula, O.: Highly light-absorbing particle emissions from low-sulfur marine fuels, npj Climate and Atmospheric Science, 9, 108, https://doi.org/10.1038/s41612-026-01369-w, 2026.

Kuebbeler, M., Lohmann, U., Hendricks, J., and Kärcher, B.: Dust ice nuclei effects on cirrus clouds, Atmos. Chem. Phys., 14, 3027–3046, https://doi.org/10.5194/acp-14-3027-2014, 2014.

Lauer, A., Eyring, V., Hendricks, J., Jöckel, P., and Lohmann, U.: Global model simulations of the impact of ocean-going ships on aerosols, clouds, and the radiation budget, Atmos. Chem. Phys., 7, 5061–5079, https://doi.org/10.5194/acp-7-5061-2007, 2007.

Lauer, A., Eyring, V., Corbett, J. J., Wang, C., and Winebrake, J. J.: Assessment of Near-Future Policy Instruments for Oceangoing Shipping: Impact on Atmospheric Aerosol Burdens and the Earth's Radiation Budget, Environ. Sci. Technol., 43, 5592–5598, https://doi.org/10.1021/es900922h, 2009.

Partanen, A. I., Laakso, A., Schmidt, A., Kokkola, H., Kuokkanen, T., Pietikäinen, J.-P., Kerminen, V.-M., Lehtinen, K. E. J., Laakso, L., and Korhonen, H.: Climate and air quality trade-offs in altering ship fuel sulfur content, Atmos. Chem. Phys., 13, 12 059–12 071, https://doi.org/10.5194/acp-13-12059-2013, 2013.

Petzold, A., Hasselbach, J., Lauer, P., Baumann, R., Franke, K., Gurk, C., Schlager, H., and Weingartner, E.: Experimental studies on particle emissions from cruising ship, their characteristic properties, transformation and atmospheric lifetime in the marine boundary layer, Atmos. Chem. Phys., 8, 2387–2403, https://doi.org/10.5194/acp-8-2387-2008, 2008.

Pope, C. A. and Dockery, D. W.: Health Effects of Fine Particulate Air Pollution: Lines that Connect, J. Air Waste Manage. Assoc., 56, 709–742, https://doi.org/10.1080/10473289.2006.10464485, 2006.

Righi, M., Hendricks, J., and Sausen, R.: The global impact of the transport sectors on atmospheric aerosol: simulations for year 2000 emissions, Atmos. Chem. Phys., 13, 9939–9970, https://doi.org/10.5194/acp-13-9939-2013, 2013.

Righi, M., Hendricks, J., Lohmann, U., Beer, C. G., Hahn, V., Heinold, B., Heller, R., Krämer, M., Ponater, M., Rolf, C., Tegen, I., and Voigt, C.: Coupling aerosols to (cirrus) clouds in the global EMAC-MADE3 aerosol–climate model, Geosci. Model Dev., 13, 1635–1661, https://doi.org/10.5194/gmd-13-1635-2020, 2020.

Righi, M., Hendricks, J., and Brinkop, S.: The global impact of the transport sectors on the atmospheric aerosol and the resulting climate effects under the Shared Socioeconomic Pathways (SSPs), Earth Syst. Dyn., 14, 835–859, https://doi.org/10.5194/esd-14-835-2023, 2023.

https://doi.org/10.5194/egusphere-2026-6471
Preprint. Discussion started: 16 November 2026
© Author(s) 2026. CC BY 4.0 License.

Roeckner, E., Brokopf, R., Esch, M., Giorgetta, M., Hagemann, S., Kornblueh, L., Manzini, E., Schlese, U., and Schulzweida, U.: Sensitivity of Simulated Climate to Horizontal and Vertical Resolution in the ECHAM5 Atmosphere Model, J. Climate, 19, 3771–3791, https://doi.org/10.1175/jcli3824.1, 2006.

Schreier, M., Mannstein, H., Eyring, V., and Bovensmann, H.: Global ship track distribution and radiative forcing from 1 year of AATSR data, Geophys. Res. Lett., 34, https://doi.org/10.1029/2007gl030664, 2007.

Seinfeld, J. H. and Pandis, S. N.: Atmospheric Chemistry and Physics: From Air Pollution to Climate Change, John Wiley & Sons, Hoboken, New Jersey, ISBN 9781119221166, 2016.

Skeie, R. B., Byrom, R., Hodnebrog, , Jouan, C., and Myhre, G.: Multi-model effective radiative forcing of the 2020 sulfur cap for shipping, Atmos. Chem. Phys., 24, 13 361–13 370, https://doi.org/10.5194/acp-24-13361-2024, 2024.

Sofiev, M., Winebrake, J. J., Johansson, L., Carr, E. W., Prank, M., Soares, J., Vira, J., Kouznetsov, R., Jalkanen, J.-P., and Corbett, J. J.: Cleaner fuels for ships provide public health benefits with climate tradeoffs, Nat. Commun., 9, https://doi.org/10.1038/s41467-017-02774-9, 2018.

Soulie, A., Granier, C., Darras, S., Zilbermann, N., Doumbia, T., Guevara, M., Jalkanen, J.-P., Keita, S., Liousse, C., Crippa, M., Guizzardi, D., Hoesly, R., and Smith, S. J.: Global anthropogenic emissions (CAMS-GLOB-ANT) for the Copernicus Atmosphere Monitoring Service simulations of air quality forecasts and reanalyses, Earth Syst. Sci. Data, 16, 2261–2279, https://doi.org/10.5194/essd-16-2261-2024, 2024.

Stengel, M., Stapelberg, S., Sus, O., Finkensieper, S., Würzler, B., Philipp, D., Hollmann, R., Poulsen, C., Christensen, M., and McGarragh, G.: Cloud_cci Advanced Very High Resolution Radiometer post meridiem (AVHRR-PM) dataset version 3: 35-year climatology of global cloud and radiation properties, Earth Syst. Sci. Data, 12, 41–60, https://doi.org/10.5194/essd-12-41-2020, 2020.

Szopa, S., Naik, V., Adhikary, B., Artaxo, P., Berntsen, T., Collins, W. D., Fuzzi, S., Gallardo, L., Kiendler-Scharr, A., Klimont, Z., Liao, H., Unger, N., and Zanis, P.: Short-Lived Climate Forcers, in: Climate Change 2021: The Physical Science Basis. Contribution of Working Group I to the Sixth Assessment Report of the Intergovernmental Panel on Climate Change, edited by Masson-Delmotte, V., Zhai, P., Pirani, A., Connors, S. L., Péan, C., Berger, S., Caud, N., Chen, Y., Goldfarb, L., Gomis, M., Huang, M., Leitzell, K., Lonnoy, E., Matthews, J., Maycock, T., Waterfield, T., Yelekçi, O., Yu, R., and Zhou, B., pp. 817–922, Cambridge University Press, Cambridge, UK and New York, NY, USA, https://doi.org/10.1017/9781009157896.008, 2021.

Twomey, S.: The Influence of Pollution on the Shortwave Albedo of Clouds, J. Atmos. Sci., 34, 1149–1152, https://doi.org/10.1175/1520-0469(1977)034<1149:tiopot>2.0.co;2, 1977.

UNCTAD: Review of Maritime Transport 2024: Navigating Maritime Chokepoints — Overview, Tech. rep., United Nations Conference on Trade and Development, Geneva, https://unctad.org/publication/review-maritime-transport-2024, 2024.

Watson-Parris, D., Christensen, M. W., Laurenson, A., Clewley, D., Gryspeerdt, E., and Stier, P.: Shipping regulations lead to large reduction in cloud perturbations, Proc. Natl. Acad. Sci., 119, https://doi.org/10.1073/pnas.2206885119, 2022.

Yi, W., Wang, X., He, T., Liu, H., Luo, Z., Lv, Z., and He, K.: The high-resolution global shipping emission inventory by the Shipping Emission Inventory Model (SEIM), Earth Syst. Sci. Data, 17, 277–292, https://doi.org/10.5194/essd-17-277-2025, 2025.

Yoshioka, M., Grosvenor, D. P., Booth, B. B. B., Morice, C. P., and Carslaw, K. S.: Warming effects of reduced sulfur emissions from shipping, Atmos. Chem. Phys., 24, 13 681–13 692, https://doi.org/10.5194/acp-24-13681-2024, 2024.

Yuan, T., Song, H., Wood, R., Wang, C., Oreopoulos, L., Platnick, S. E., von Hippel, S., Meyer, K., Light, S., and Wilcox, E.: Global reduction in ship-tracks from sulfur regulations for shipping fuel, Sci. Adv., 8, eabn7988, https://doi.org/10.1126/sciadv.abn7988, 2022.

https://doi.org/10.5194/egusphere-2026-6471
Preprint. Discussion started: 16 November 2026
© Author(s) 2026. CC BY 4.0 License.



Yuan, T., Song, H., Oreopoulos, L., Wood, R., Bian, H., Breen, K., Chin, M., Yu, H., Barahona, D., Meyer, K., and Platnick, S.: Abrupt reduction in shipping emission as an inadvertent geoengineering termination shock produces substantial radiative warming, Commun. Earth Environ., 5, https://doi.org/10.1038/s43247-024-01442-3, 2024.

615 Zhang, F., Xiao, B., Liu, Z., Zhang, Y., Tian, C., Li, R., Wu, C., Lei, Y., Zhang, S., Wan, X., Chen, Y., Han, Y., Cui, M., Huang, C., Wang, H., Chen, Y., and Wang, G.: Real-world emission characteristics of VOCs from typical cargo ships and their potential contributions to secondary organic aerosol and O3 under low-sulfur fuel policies, Atmos. Chem. Phys., 24, 8999–9017, https://doi.org/10.5194/acp-24-8999-2024, 2024.